Introduction

Circadian clocks operate at the transcriptional level across diverse organisms, producing distinct gene networks that oscillate on a 24 h cycle (Kulshrestha & Devkar, 2023). In mammals, the molecular mechanism of the circadian clock is driven by a cell-autonomous transcriptional autoregulatory feedback loop wherein; the core clock genes comprise of CLOCK and BMAL1 (activators), and PER1, PER2, CRY1, and CRY2 (repressors) (Isojima et al., 2003). Studies in the previous decade have shed light on the genomic targets of the core clock pathway, revealing the extensive influence of circadian regulation on gene expression (Mazzoccoli et al., 2012). A significant proportion (~5-20%) of genes in any given cell or tissue exhibit circadian oscillations at the mRNA level (Ptitsyn et al., 2006). However, this regulation in gene expression is just one of the many layers of circadian control (Guan & Lazar, 2022). Studies have revealed that nearly every stage of gene expression viz., transcription (Panda et al., 2002), splicing (Sanchez et al., 2010), termination (Padmanabhan et al., 2012), polyadenylation (Kojima et al., 2012), nuclear export (Vielhaber et al., 2001), miRNA regulation (X. Wang et al., 2015), and RNA degradation (Torres et al., 2018)is subject to circadian control. Thus, both transcriptional and post-transcriptional regulation play crucial roles in controlling circadian gene expression (Torres et al., 2018).

Nocturnin (Noct) is a circadian deadenylase that regulates gene expression by removing poly(A) tails from its target mRNAs (Baggs & Green, 2003). Further, Noct is robustly rhythmic in liver and this property implies towards its involvement in circadian processes (Onder et al., 2019). Though Noct is not directly involved in regulating expression of the core clock genes, it does have functions in mediating its rhythmic output (Kulshrestha & Devkar, 2023). Since many rate-limiting enzymes in metabolic reactions are regulated by the circadian clock, gene expression needs to be precisely controlled, with post-transcriptional mechanisms such as deadenylation playing a crucial role in this regard (X. Yao et al., 2020). In humans and mice, the core clock genes (Bmal1 and Clock) are recruited to the E-box transcriptional element in the Noct promoter. Studies have demonstrated that CLOCK and BMAL1 interact with the *Noct* promoter in Huh7

hepatoma cells, influencing its expression independent of circadian time (Li et al., 2008a). Similarly, in liver samples from CLOCK mutant mice, *Noct* expression maintained rhythmicity but with reduced amplitude (Stubblefield et al., 2012). Another study reported a time-dependent association of BMAL1 with the *Noct* promoter in wild-type mice (Rey et al., 2011). Thus, systemic signals, possibly those related to feeding and nutrient metabolism, also play a key role in regulating Noct expression (Douris & Green, 2008). Furthermore, these findings suggest several mechanisms by which the circadian clock regulates *Noct* mRNA expression, including BMAL1-CLOCK dimer formation (Li et al., 2008), subsequent CREB phosphorylation, and binding of phosphorylated CREB (pCREB) to the Nocturnin Element (NE) of the *Noct* promoter (Green & Liu, 2002).

Studies in Noct knock out (*Noct* $^{-/-}$) mice have shown that hepatic *Noct* is robustly rhythmic and fasting, re-feeding and chronic HFD consumption greatly influence *Noct* expression and rhythmicity (Stubblefield et al., 2018). Additionally, transcriptomic analysis of liver tissues of WT and *Noct* $^{-/-}$ mice revealed that the mRNAs exhibiting an increased fold-change amplitude in the *Noct* $^{-/-}$ liver were significantly enriched in those related to cholesterol and lipid metabolism. These mRNAs encoded proteins that play a crucial role in the general metabolic flux pathway for producing acetyl CoA, cholesterol and triglycerides. Moreover, these mRNAs recorded heightened amplitude in *Noct* $^{-/-}$ livers during the dark phase at ZT12, coinciding with the peak expression of NOCT protein in WT mice (Stubblefield et al., 2018). Thus, these findings implied that these mRNAs involved in hepatic lipid metabolism, could be direct targets of the deadenylase activity of Noct. Further, an altered hepatic Noct expression could culminate in the initiation of NAFLD/NASH. However, detailed studies in this regard are lacking.

Computational tools such as differential gene expression analysis (DGEA) of GEO datasets from NCBI are a vital tool for identifying potential targets of an enzyme by assessing alterations in gene expression profiles in response to enzyme activity (S. Yao & Liu, 2018). When an enzyme is overexpressed, knocked down,

or inhibited, the resultant changes in the transcriptome can reveal downstream effects on gene regulation. Thus, by comparing expression levels in experimental conditions with those of control groups, researchers can pinpoint differentially expressed genes (DEGs) that may be directly or indirectly influenced by the enzyme in question (A. Wang & Zhang, 2017). Statistical methods, such as DESeq2 or edgeR, are commonly employed to analyse high-throughput data from techniques such as RNA sequencing or microarrays, providing robust evidence of significant expression changes (Rosati et al., 2024). These DEGs can then be subjected to functional enrichment analysis to uncover biological pathways that are modulated by the enzyme, aiding in elucidating its role within metabolic networks. Hence, this approach not only identifies potential substrate interactions but also aids in understanding the broader biological implications of enzyme activity (A. Wang & Zhang, 2017).

This chapter employs *in silico* tools such as DEG analysis to identify the potential targets of Nocturnin. In addition, hepatic Noct oscillations shall be scrutinized in H and/or CD induced NASH mouse model and in HepG2 cells to establish the circadian basis of Noct in NASH pathology.

Methodology

Computational studies

Differential gene expression analysis (DGEA) was performed for the GEO dataset (GSE123477) that comprised of RNA-Seq data of WT and *Noct*$^{-/-}$ cells. The differentially expressed genes (DEGs) were subjected to enrichment analysis to identify the potential targets of Noct.

In vivo studies

Male C57BL/6J mice were subjected to high-fat-high-fructose (H) diet alone or in combination with photoperiodic shifts induced chronodisruption (CD) for 16 weeks. At the end of 16 weeks, mice were euthanized and liver tissues were harvested at 5 timepoints (ZT=0,6,12,18 and 24). Experimental groups:

1. Control (C)
2. High-fat-high-fructose diet (H)
3. Chronodisruption (CD)
4. High-fat-high-fructose diet + Chronodisruption (CD)

In vitro studies

HepG2 cells were serum-synchronized and subjected to oleic acid (OA) alone for 24 h. Subsequently, cells were collected at different time points for gene and protein expression studies.

Parameters

1. Cytotoxicity analysis to standardize concentration of OA.
2. ORO staining to assess intracellular lipid accumulation.
3. Gene expression studies by qPCR: *mmu-Noct* and *hsa-NOCT* oscillations.
4. Protein expression studies by Western Blotting: hsa-NOCT oscillations.
5. CircWave analysis to scrutinize Noct rhythmicity.

Methodology:

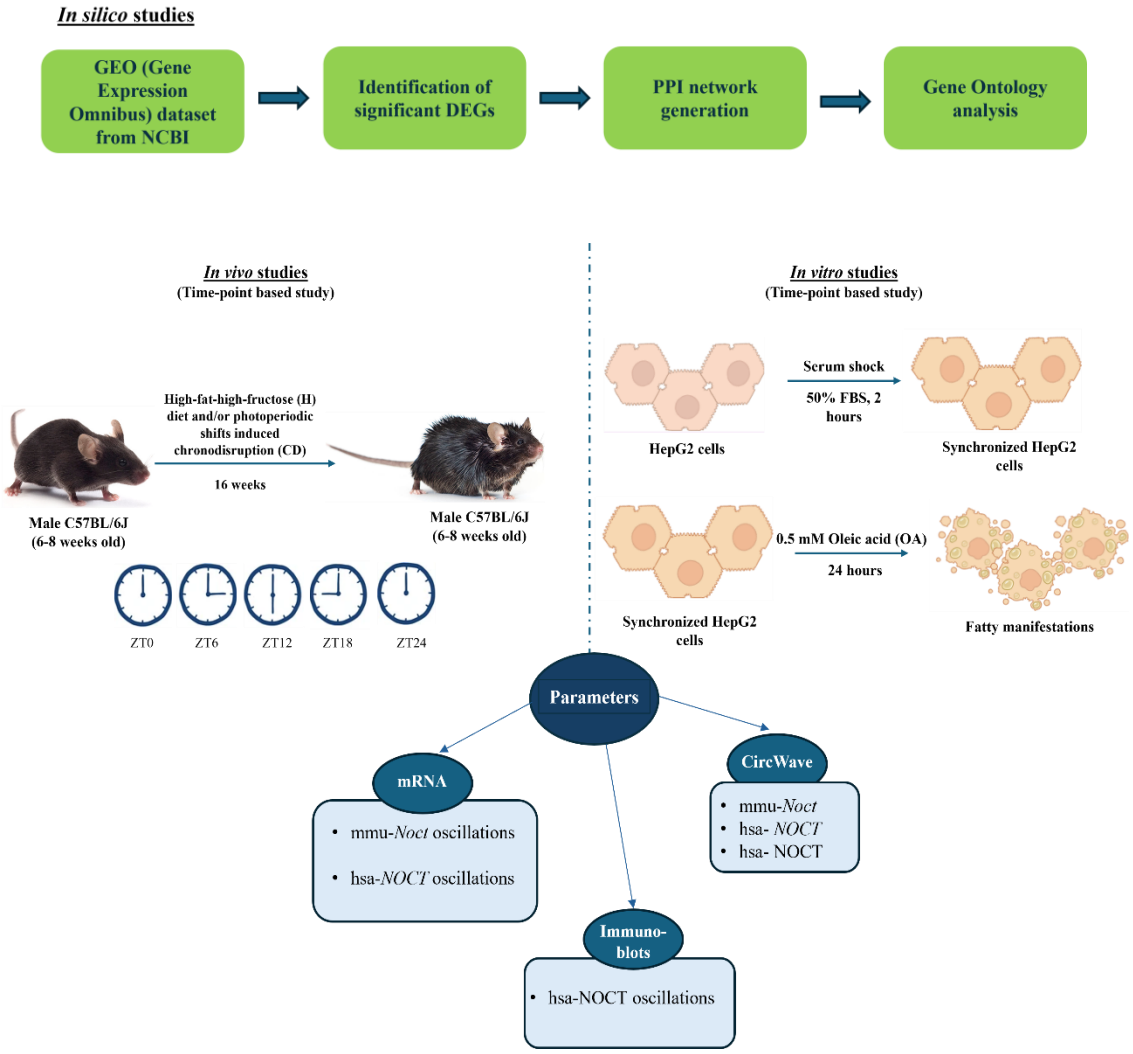

The detailed experimental regime and parameters for in vivo model validation have been outlined in the Materials and Methods section.

Results:

In silico analysis identified Nocturnin (Noct) as a key regulator of hepatic lipid metabolism.

To understand key functions of Noct in liver, differential gene expression analysis (DGEA) was performed. Gene expression profiling data with the series number GSE123477 was procured from the Gene Expression Omnibus (GEO) database. The data comprised of 2 samples, each of wildtype (WT) and Noct knockout (Noct KO) A549 cells. Box plot [Fig. 1.1 (a)] showed that the data values were normalized and cross-comparable. DGEA was performed using GEO2R. Out of 17,428 genes, 71 genes differentially expressed [Fig. 1.1(b)]. The distribution of differentially expressed genes (DEGs) was visualized in a volcano plot using false discovery rate (FDR<0.05) and |logFC | >1 as screening criteria [Fig.1.1 (c)]. Further, significantly upregulated or downregulated genes were depicted by red or blue dots, respectively.

The DEGs were subjected to gene ontology (GO) analysis in Webgestalt server wherein; biological processes (such as regulation, response to stimulus) [Fig. 1.2 (a)], cellular component categories (such as membrane, membrane enclosed lumen) [Fig. 1.2 (b)] and molecular functions such as protein and ion binding [Fig. 1.2 (c)] were significantly enriched. Further, normalized enrichment scores revealed processes such as lipid metabolism regulation and response to xenobiotic stimulus to be significantly upregulated whereas, processes such as angiogenesis and positive regulation of response to external stimulus to be significantly downregulated [Fig. 1.2 (d)]. With protein-protein interaction (PPI) analysis using STRING software, key metabolic genes such as HNF4A and SCD were identified [Fig. 1.3].

High-fat-high-fructose (H) diet alone or in combination with photoperiodic shifts induced chronodisruption (CD) alters hepatic *Noct* expression at ZT12.

Male C57BL/6J mice subjected to high-fat-high-fructose (H) diet alone or in combination with photoperiodic manipulations induced chronodisruption (CD) for 16 weeks were marked by significantly increased circulating titres of serum liver function markers (ALT and AST), lipid profile as well as intrahepatic lipid accumulation [Fig. M2 and M3]. These alterations were accompanied by significant increments in hepatic *Noct* expression at ZT12 wherein; H group recorded highest expression ($p<0.001$). CD and HCD groups recorded a moderate, albeit significant increment ($p<0.05$ and $p<0.001$ respectively) [Fig. 1.4].

Hepatic *Noct* mRNA expression is altered in mice subjected to high-fat-high-fructose (H) diet and/or photoperiodic shifts induced chronodisruption (CD).

Possible aberrations in hepatic *Noct* mRNA oscillations in control and experimental mice were assessed by harvesting liver tissues at five timepoints (ZT0, 6, 12, 18 and 24). In control (C) mice, hepatic *Noct* expression recorded dampened expression except at ZT12 that was evident by a 4-fold increase at the said timepoint. H group recorded significant increment in *Noct* mRNA at ZT12 ($p<0.05$) and a moderate increment at ZT18 ($p<0.05$) whereas, CD and HCD groups recorded significant increments ZT6 ($p<0.01$ and $p<0.05$ respectively) and dampened expression at the remaining timepoints [Fig. 1.5].

High-fat-high-fructose (H) diet and/or chronodisruption (CD) alter the rhythmicity of *Noct* mRNA.

To assess possible changes in *Noct* rhythmicity, the data was analysed in CircWave software wherein data was plotted as a combinatory sine-cosine wavefunction and was further scrutinized using parameters such as percentage (%) relative amplitude, peak time (represented as "Centre of Gravity- CoG), and cumulative *Noct* expression (*Noct* expression over a period of 24 hours). H and HCD groups recorded a non-significant increment in the % relative amplitude whereas, CD group recorded a significant increment ($p<0.05$) [Fig. 1.6 (b)]. Further, H group recorded CoG at ZT12. On the other hand, CD and HCD groups recorded shifts from ZT12 to ZT6 [Fig. 1.6 (c)]. A significant increment ($p<0.001$) in the

cumulative *Noct* expression was observed in H and HCD groups whereas, CD group recorded a non-significant increment [Fig. 1.6 (d)].

Oleic acid (OA) treatment attenuated cell viability in HepG2 cells and accounted for intracellular lipid accumulation.

HepG2 cells were treated with increasing concentrations of OA (0.5 mM- 2 mM) for 24 h and cell viability was assessed by MTT assay. A dose-dependent decrement in cell viability was observed in OA-treated groups wherein; the highest concentration of OA (2 mM) recorded minimum number of cells and on the basis of the cell viability results, 0.5 mM concentration was selected for further experiments [Fig. 1.7 (a)]. Further, HepG2 cells subjected to 0.5 mM OA for 24 h recorded a significant accumulation of intracellular lipids, as quantified by Oil Red O (ORO) staining [Fig. 1.7 (b)].

Oleic acid (OA) treated-HepG2 cells record elevated Noct expression.

HepG2 cells were subjected to serum-shock treatment for 2 h to synchronize their individual circadian clocks, followed by treatment with 0.5 mM OA for 24 h. OA-treated HepG2 cells recorded a significant increase in *NOCT* mRNA expression [Fig. 1.7 (a)]. Further, immunoblots revealed a concomitant increment in NOCT protein expression as well [Fig. 1.7 (b) and (c)].

Oleic acid (OA) treatment alters *NOCT* mRNA expression and rhythmicity in HepG2 cells.

Serum synchronized HepG2 cells were subjected to 0.5 mM of OA for 24 h and subsequently, the cells were harvested at different time points (24 h, 28 h, 32 h, 36 h, 40 h, 44 h and 48 h) for assessing Noct mRNA and protein oscillations. Control HepG2 cells showed consistently low *NOCT* expression at all time points, with a relatively higher expression observed at 36 h. In contrast, OA treatment accounted for a significant increment in *NOCT* expression at 36 h ($p<0.05$), followed by a decrement at 40 h [Fig. 1.8].

CircWave analysis corroborated with these findings [Fig. 1.9 (a)], revealing a significant increment in the percentage relative amplitude of *NOCT* ($p<0.01$) in

the OA-treated group [Fig. 1.9 (b)]. Additionally, OA-treated HepG2 cells exhibited a shift in the centre of gravity (CoG) from 36 h to 32 h [Fig. 1.9 (c)] . The cumulative *NOCT* expression was also significantly elevated ($p<0.05$) in OA-treated HepG2 cells [Fig. 1.9 (d)].

Oleic acid (OA) treatment alters NOCT protein oscillations in HepG2 cells.

Immunoblots of Control HepG2 cells revealed dampened NOCT oscillations at all time points, with a moderate peak observed at 48 h. Treatment with 0.5 mM OA caused the peak to shift from 48 h to 36 h ($p<0.001$) whereas, NOCT expression at other time points, namely 24 h ($p<0.01$), 32 h ($p<0.001$) and 48 h ($p<0.01$) was significantly lower in the OA-treated group compared to the control [Fig. 1.10 (a) and (b)].

These findings were supported by the CircWave analysis that recorded a significant alteration in NOCT rhythmicity evident from the combinatory sine-cosine wavefunction [Fig. 1.11 (a)] as well as a significant increment ($p<0.01$) in the % relative amplitude in OA group [Fig. 1.11 (b)]. Further, the centre of gravity (CoG) was shifted to ~36 h in OA treated group [Fig. 1.11 (c)]. However, the cumulative NOCT protein showed a non-significant decrement in the OA group as compared to the control [Fig. 1.11 (d)].

(a)

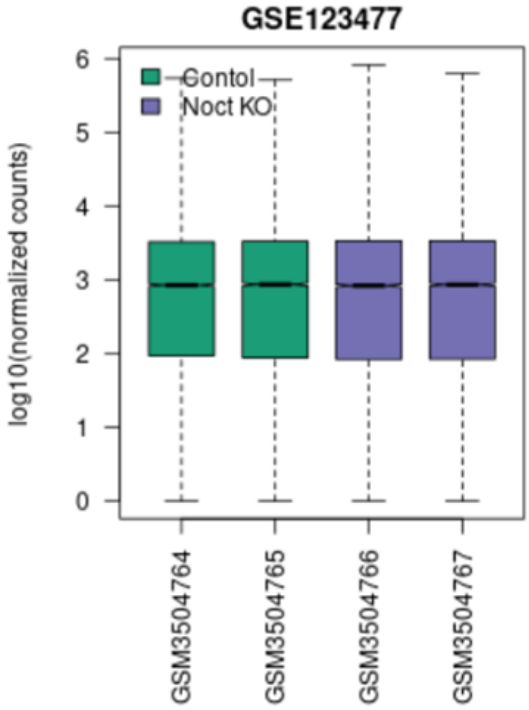
GSE123477
Contol
Noct KO
log10(normalized counts)
0
1
2
3
4
5
6
GSM3504764
GSM3504765
GSM3504766
GSM3504767

(b)

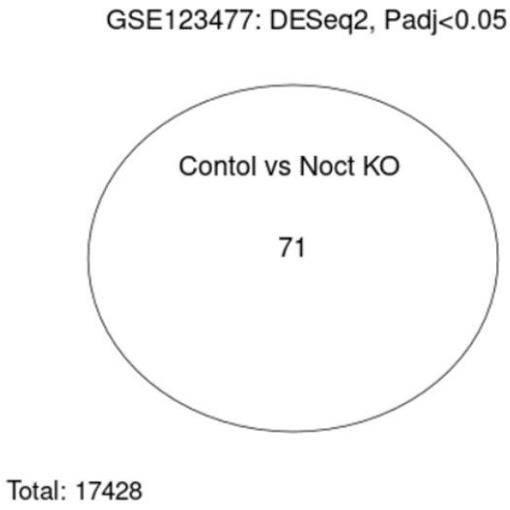
GSE123477: DESeq2, Padj<0.05
Contol vs Noct KO
71
Total: 17428

(c)

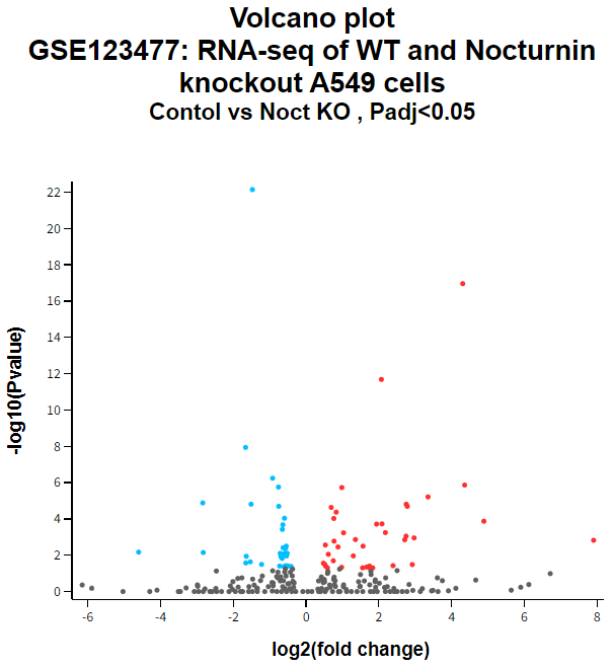

Figure 1.1. Differential Gene Expression Analysis (DGEA) of wildtype (WT) and Noct knockout (*Noct*$^{-/-}$) A549 cells from RNA-seq data retrieved from Gene Expression Omnibus (GEO; GSE123477): (a) Box plot of the datasets; (b) Venn diagram depicting the differential genes and (c) Volcano plot of the differentially expressed genes wherein; the red dots indicate upregulated genes and the blue dots indicate down-regulated genes.

(a)

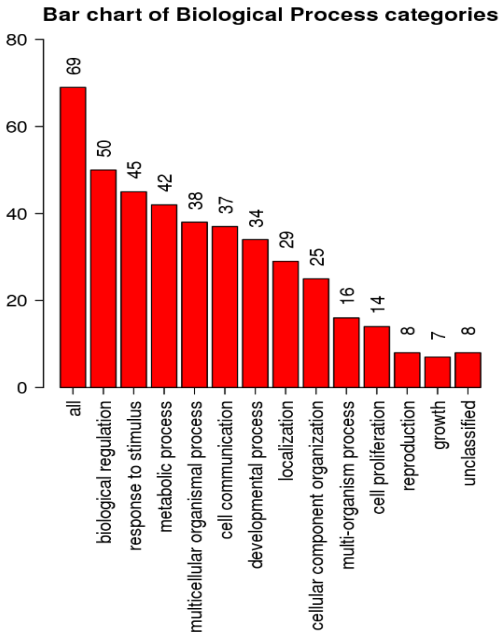
Bar chart of Biological Process categories
80
60
40
20
0
69
50
45
42
38
37
34
29
25
16
14
8
7
8
all
biological regulation
response to stimulus
metabolic process
multicellular organismal process
cell communication
developmental process
localization
cellular component organization
multi-organism process
cell proliferation
reproduction
growth
unclassified

(b)

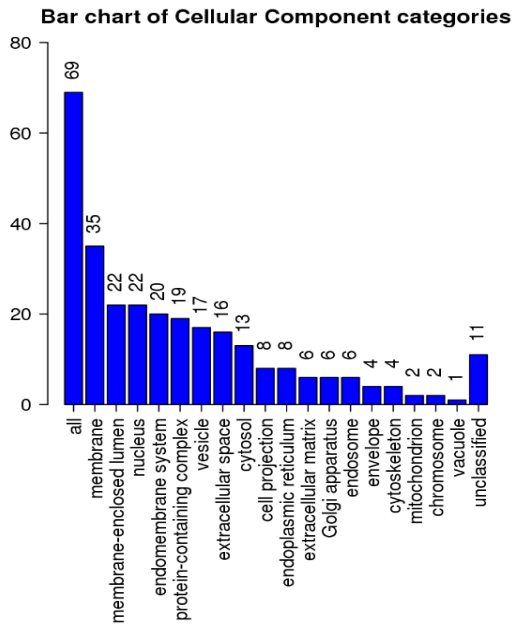
Bar chart of Cellular Component categories
80
60
40
20
0
69
35
22
22
20
19
17
16
13
8
8
6
6
6
4
4
2
2
1
11
all
membrane
membrane-enclosed lumen
nucleus
endomembrane system
protein-containing complex
vesicle
extracellular space
cytosol
cell projection
endoplasmic reticulum
extracellular matrix
Golgi apparatus
endosome
envelope
cytoskeleton
mitochondrion
chromosome
vacuole
unclassified

(c)

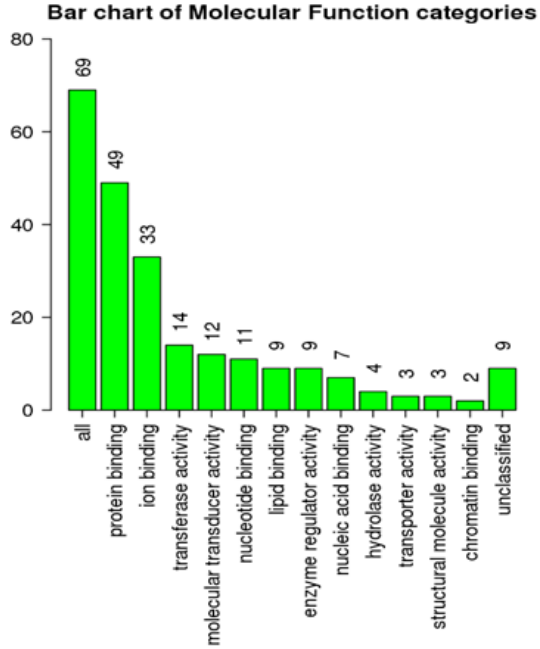
Bar chart of Molecular Function categories
80
60
40
20
0
69
49
33
14
12
11
9
9
7
4
3
3
2
9
all
protein binding
ion binding
transferase activity
molecular transducer activity
nucleotide binding
lipid binding
enzyme regulator activity
nucleic acid binding
hydrolase activity
transporter activity
structural molecule activity
chromatin binding
unclassified

(d)

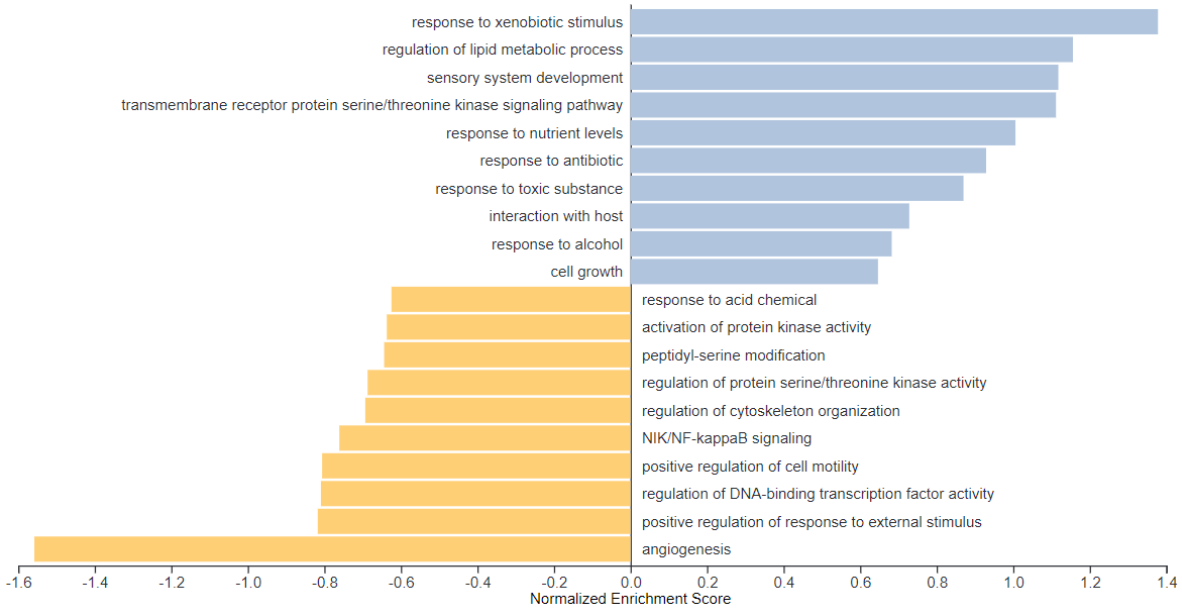

Figure 1.2. Gene ontology (GO) analysis of the differentially expressed genes: genes enriched in (a) biological processes; (b) cellular components and (c) molecular functions; (d) Normalized enrichment scores of genes enriched in various physiological processes.

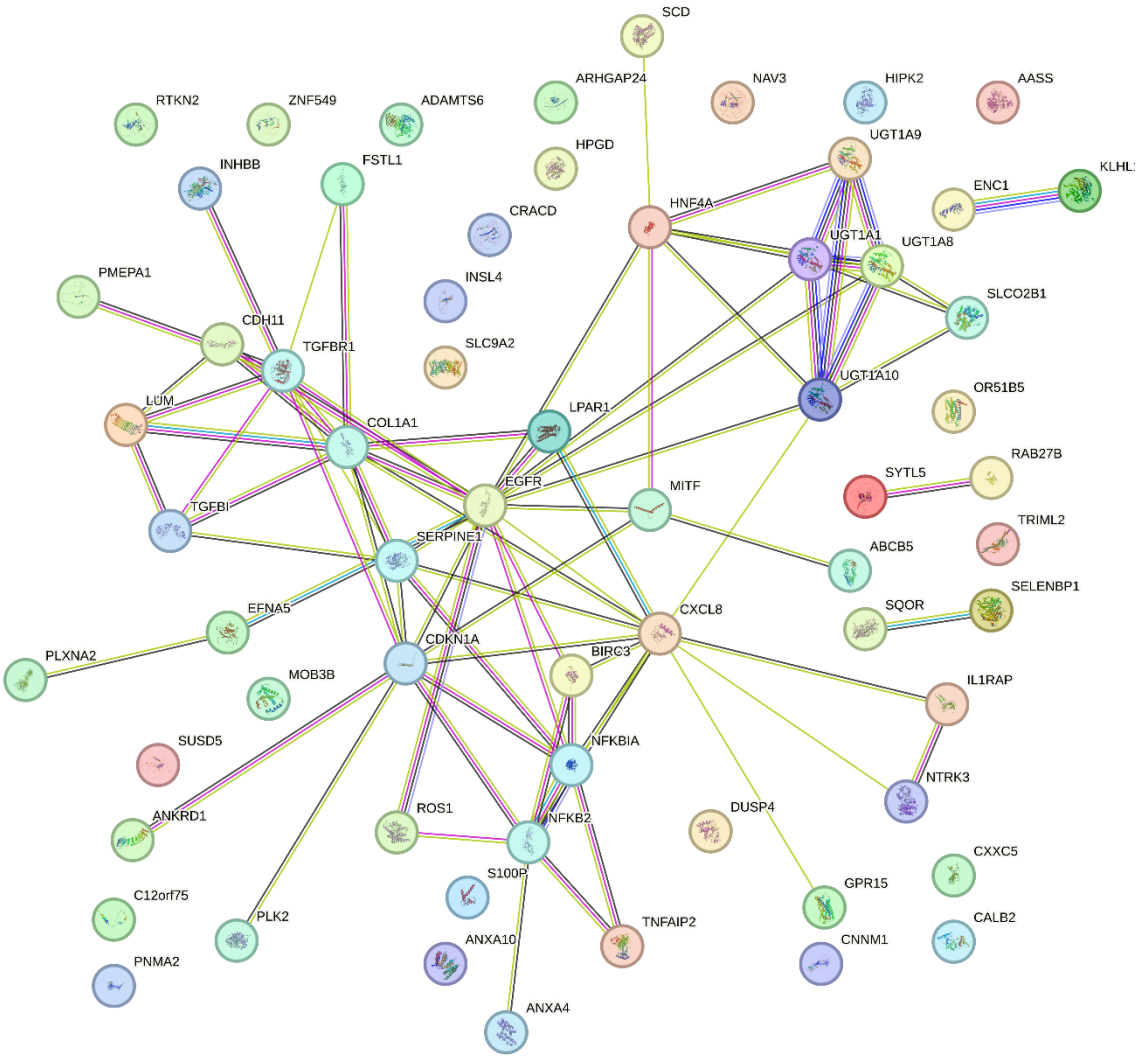

Figure 1.3 STRING network analysis identified DEGs. The colored nodes represent query proteins and first shell of interactors, and the white nodes represent the second shell of interactors.

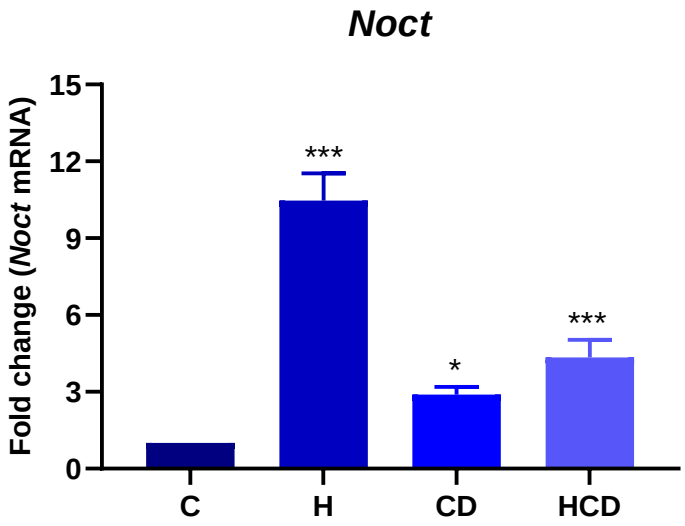

Figure 1.4. Alterations in *Noct* mRNA (at ZT12) in the livers of C57BL/6J mice subjected to high-fat-high-fructose (H) diet and/or photoperiodic manipulations induced chronodisruption (CD) regime for 16 weeks. Results are represented as mean ± SD. *p<0.05 and ***p<0.001 when H, CD and HCD groups are compared with Control (C).

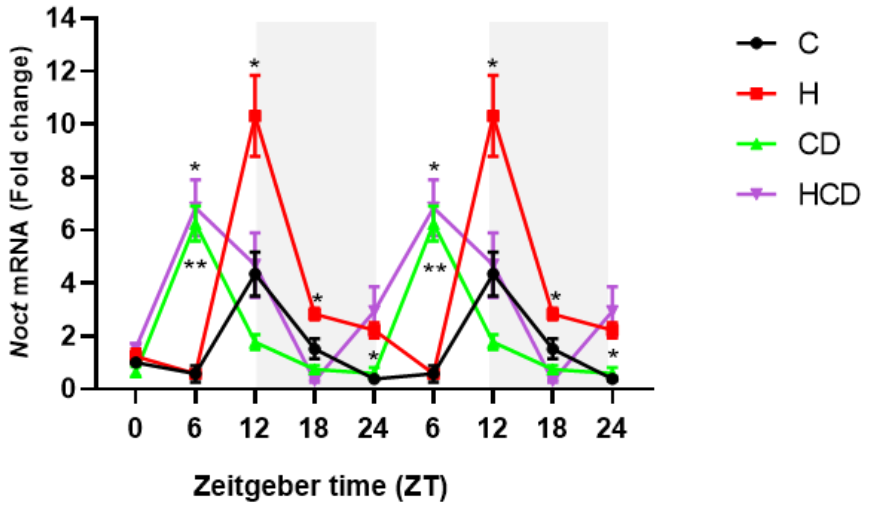

Figure 1.5. High-fat-high-fructose (H) diet alone and/or photoperiodic manipulations induced chronodisruption (CD) for 16 weeks alters hepatic *Noct* mRNA oscillations in C57BL/6J mice. Grey shaded region indicates dark phase. n= 3 for each time point. Results are presented as mean ± SD. *p<0.05 and **p<0.01 when H, CD and HCD groups are compared to Control (C).

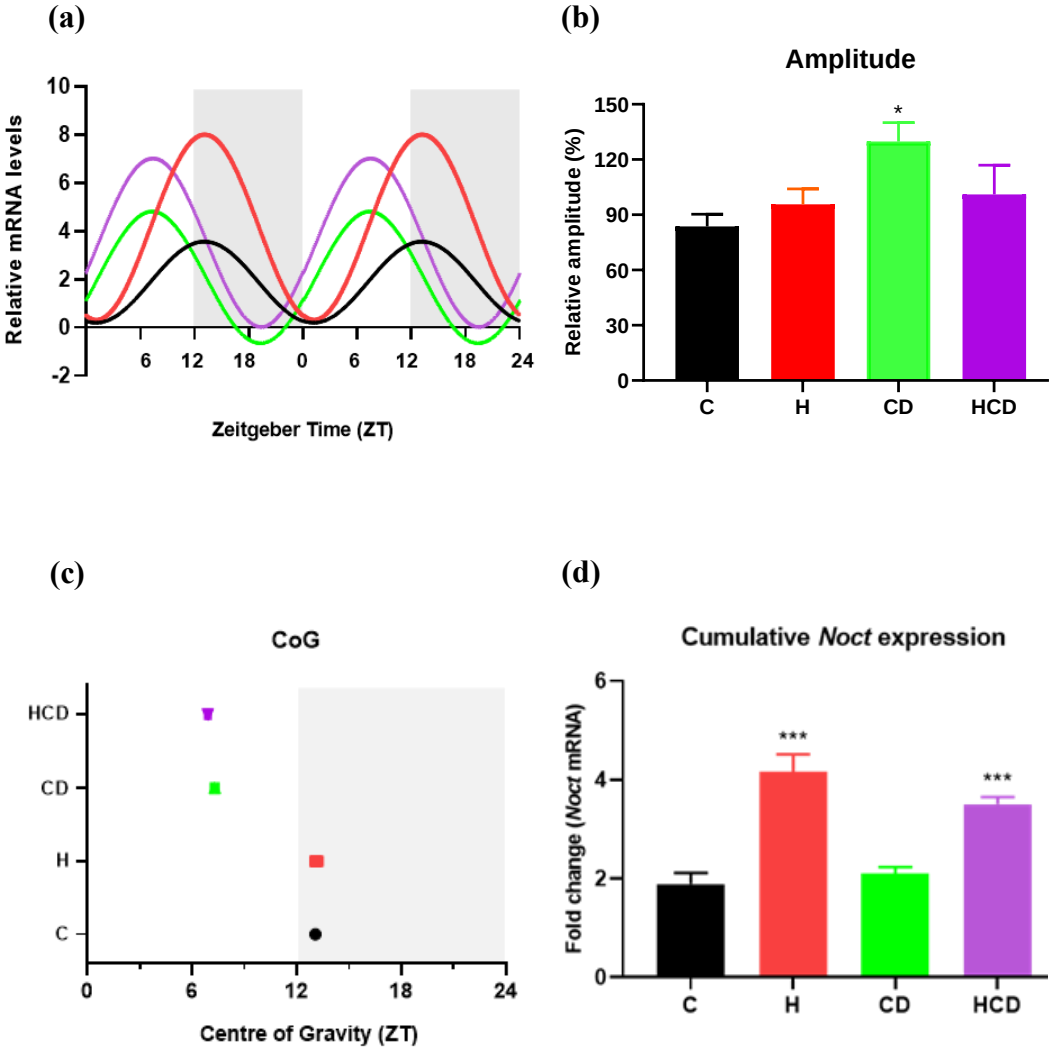

Figure 1.6. CircWave analysis of hepatic *Noct* mRNA rhythmicity in H and/or CD mice (a) *Noct* mRNA oscillations in the form of a combinatory sine-cosine wave-function; (b) Relative percentage (%) amplitude of *Noct* mRNA; (c) Peak time (represented in the form of "Centre of Gravity -CoG") and (d) Cumulative *Noct* expression over a period of 24 h. Results are presented as mean ± SD. *p<0.05 and ***p<0.001 when H, CD and HCD groups are compared with Control (C).

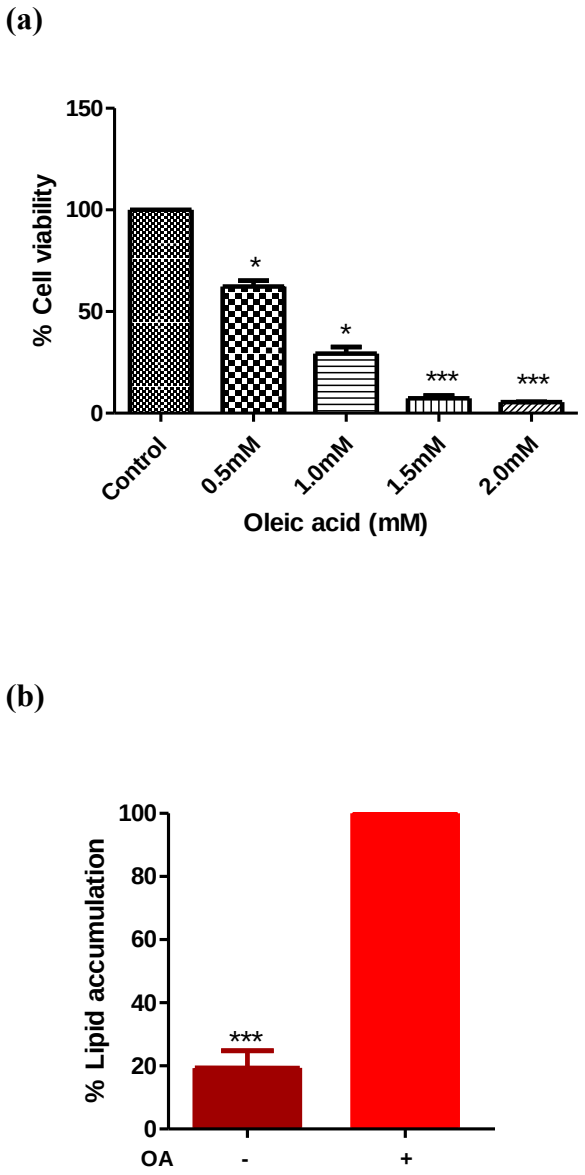

Figure 1.7. Oleic acid (OA) treatment imparts fatty manifestations in HepG2 cells: (a) Dose standardization of OA by MTT assay and (b) Intracellular lipid accumulation quantified by Oil Red O (ORO) staining. Results are expressed as mean ± SD (n=3). *p<0.05, ***p<0.001 when OA group is compared with Control.

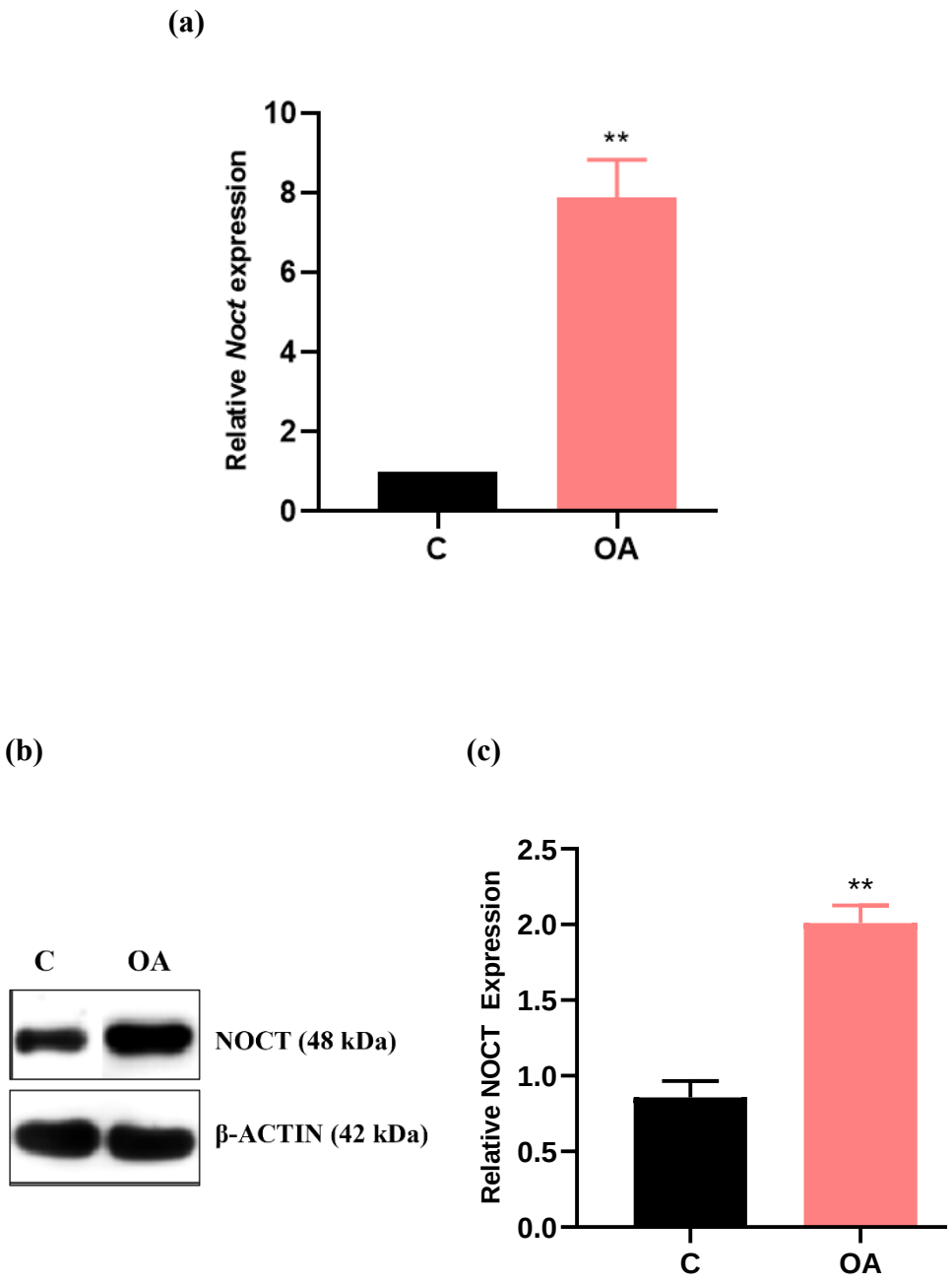

Figure 1.8. Oleic acid (OA; 0.5 mM) treatment for 24 h significantly increases Noct expression in HepG2 cells: (a) mRNA expression of *NOCT*; (b) immunoblots of NOCT protein in Control (C) and OA group and (c) relative NOCT protein expression. Results are presented as mean ± SD (n=3). **p<0.01 when OA group is compared with C.

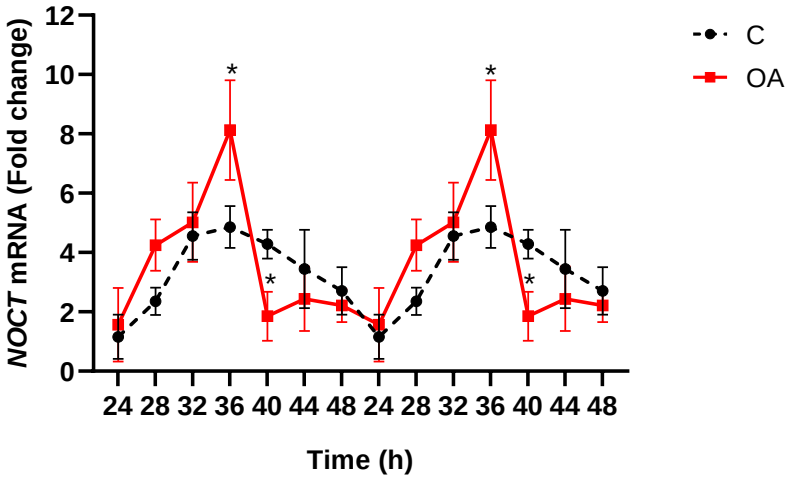

Figure 1.9. Serum synchronized HepG2 cells were subjected to 0.5 mM oleic acid (OA) for 24 h and *NOCT* mRNA levels were assessed at different time points. Results are expressed as mean ± SD; n= 3. *p<0.05 when OA group is compared with control (C).

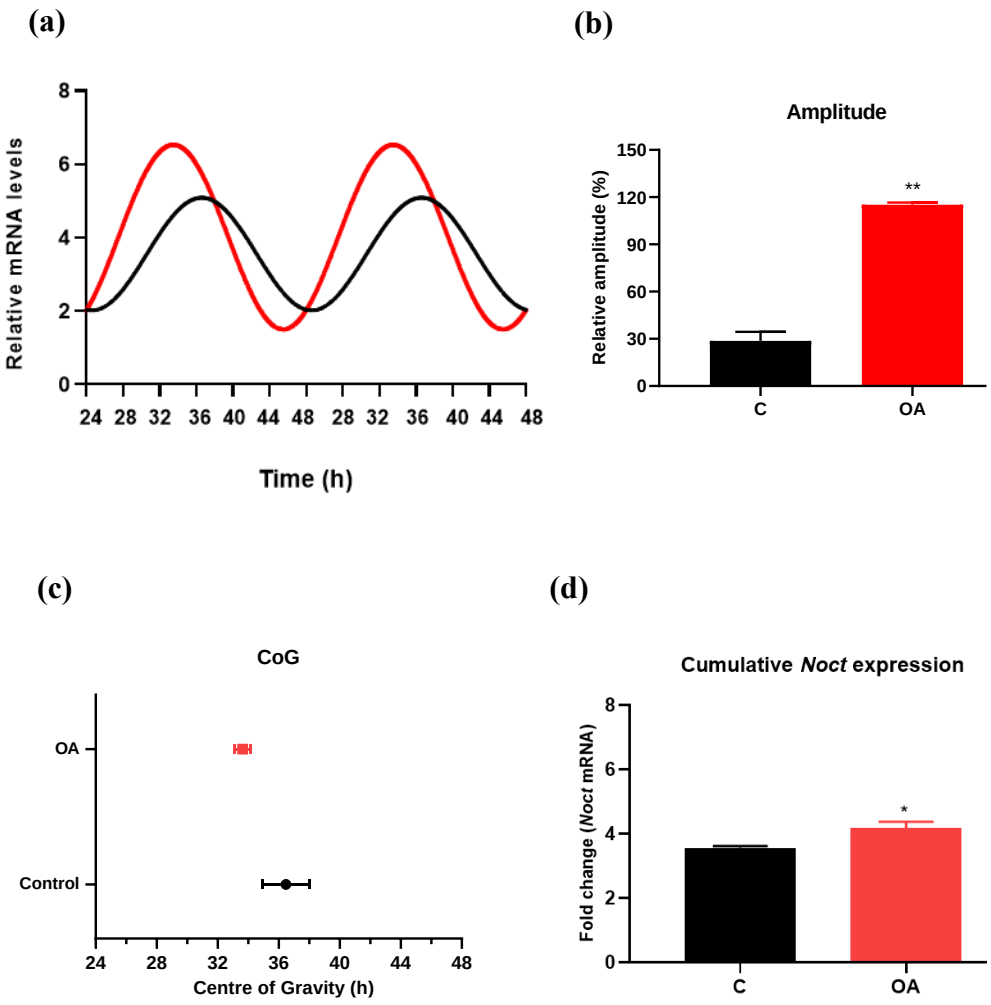

Figure 1.10. CircWave analysis of *NOCT* oscillations in serum synchronized HepG2 cells subjected to OA treatment for 24 h: (a) *NOCT* oscillations in the form of a sine-cosine wave-function; (b) Relative % amplitude; (c) Peak time represented in the form CoG and (d) Cumulative *NOCT* expression. Black color indicates control group and Red indicates OA group. Results are presented as mean ± SD. *$p<0.05$ and **$p<0.01$ when OA group is compared with Control (C).

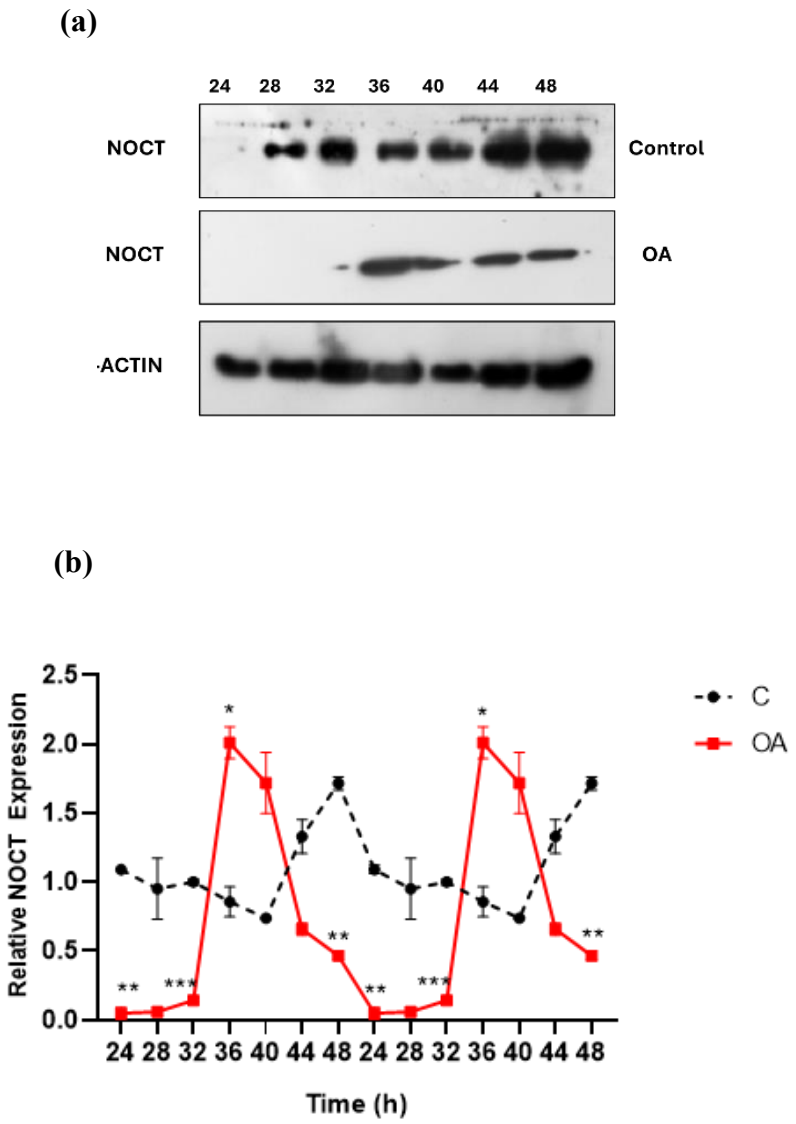

Figure 1.11. Immunoblot analysis of NOCT protein oscillations in serum-synchronized HepG2 cells subjected to OA treatment for 24 h. (a) Immunoblots of NOCT protein at different time points (b) NOCT protein oscillations in Control and OA group. Results are expressed as mean ± SD; n=3 at each time point. *p<0.05, **p<0.01 and ***p<0.001 when OA group is compared with Control (C).

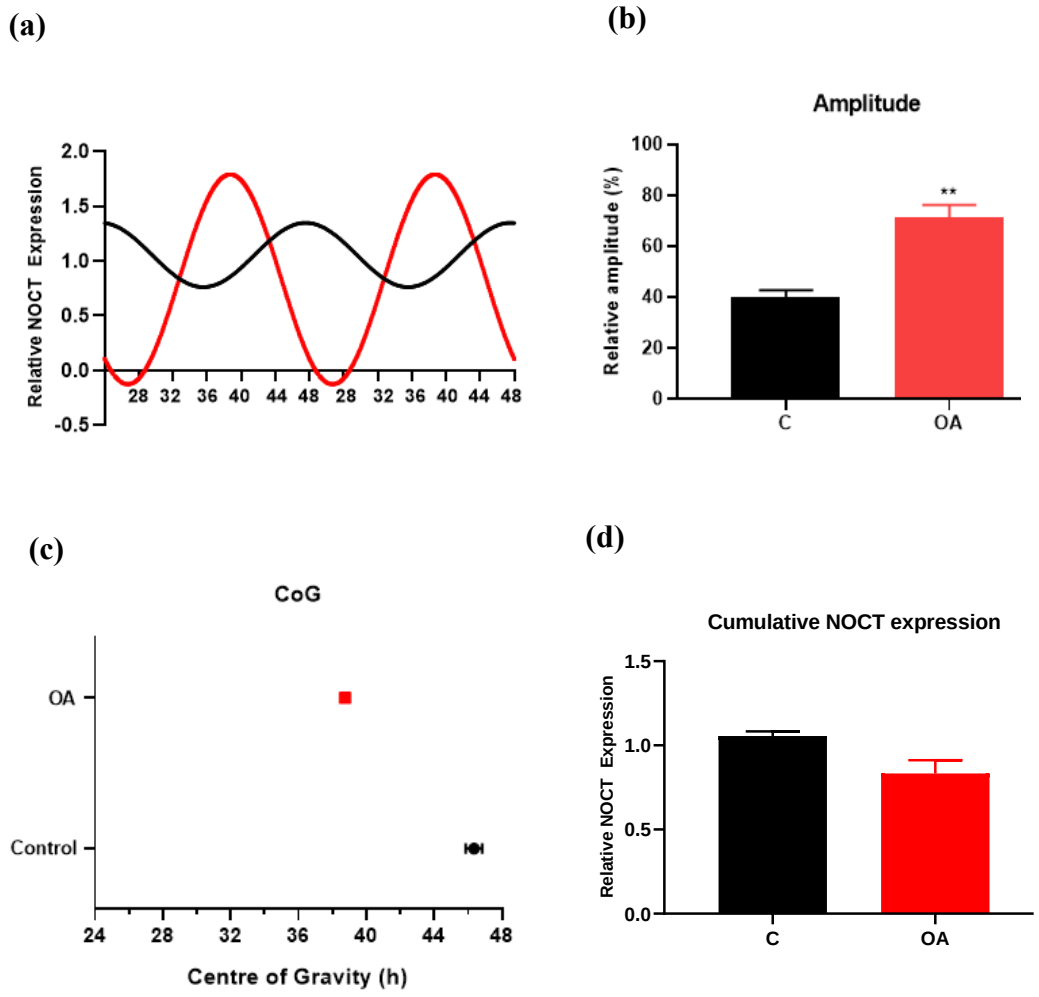

Figure 1.12. Rhythmicity of NOCT protein Control (C) and OA groups analyzed by CircWave software: (a) NOCT oscillations in the form of a sine-cosine wavefunction; (b) Relative % amplitude; (c) Peak time represented as CoG and (d) Cumulative NOCT expression. Black color indicates control group and Red indicates OA group. Results are expressed as mean ± SD. **p<0.01 when OA group is compared with Control.

Discussion:

Nocturnin (Noct) is a metabolically relevant circadian clock output that is robustly rhythmic in liver (Laothamatas et al., 2020). Noct functions as a deadenylase and regulates gene expression by virtue of its rhythmic deadenylase activity (Nishikawa et al., 2013). Studies involving Noct knockout (*Noct*$^{-/-}$) mice had implied towards its possible role in regulating hepatic cholesterol and TG metabolism. Another study had revealed that the rhythmicity and amplitude of hepatic *Noct* mRNA were altered by fasting and re-feeding paradigms, especially by chronic HFD consumption (Stubblefield et al., 2018). These findings suggest that Noct is responsive to nutritional challenges and point to its essential role in regulating hepatic lipid metabolism. However, mechanistic insights into the regulatory role of Noct remain largely unknown. Further, it shall be interesting to investigate the status of Noct expression in lifestyle disorders. The present study delves into elucidating the possible targets of Noct and understanding its role in diet and/or CD induced NASH pathology.

In order to identify the possible target mRNAs of Noct, we analysed the differential expression between wild-type (WT) and *Noct*$^{-/-}$ cells using RNA-seq profiling data with multiple bioinformatic tools such as enrichment analysis and PPI analysis. Herein, based on the GEO database, we analysed and integrated the RNA-seq data using the software package, and the resultant 71 differentially expressed genes were further scrutinized with STRING. PPI analysis with the differential genes revealed that *HNF4A, SCD, NFKB1A* and *NFKB2* are the potential targets of Noct. Various studies have linked altered expression of *HNF4A* to NASH pathophysiology. Mice with liver-specific ablation of *Hnf4a* displayed steatotic liver and impaired hepatic glucose metabolism. Additionally, defects in HDL metabolism and hepatic steatosis were reported in these mice (Thymiakou et al., 2023). In another study, computational analyses identified *HNF4A* as a key player in NASH (Baciu et al., 2017). *SCD-1* is a key lipogenic gene in the liver and studies have shown that higher expression of *SCD-1* correlates with hepatic fatty manifestations and hepatic steatosis (Kurikawa et al., 2013). In a study, inhibiting *SCD* activity imparted resistance against diet-induced obesity,

metabolic syndrome and NASH and improved glucose and insulin tolerance (Q. Sun et al., 2024). Our computational analysis further revealed lipid metabolism as one of the key pathways significantly enriched. Thus, identification of key metabolic genes such as *HNF4A* and *SCD* as potential targets of Noct, provides important clues about the regulatory role of Noct in liver.

Herein, male C57BL/6J mice were subjected to high-fat-high-fructose (H) diet and/or photoperiodic manipulations induced chronodisruption (CD) for 16 weeks. This served as an *in vivo* model of NASH and this experimental setup simulates conditions of a lifestyle disorder and is an established animal model in our laboratory. Significant increments in body weight, liver weight and body-to-liver weight ratios were recorded in H and HCD groups, whereas CD group recorded a moderate increment. Additionally, H, CD and HCD groups exhibited significant elevations in serum liver function markers (ALT and AST) and serum lipid profile parameters, suggestive of liver damage. Histological analysis revealed a marked increment in intrahepatic lipid accumulation in liver tissues of these groups, accompanied by elevated steatosis scores and ballooning hepatocytes, confirming fatty liver manifestations. Furthermore, the mRNA levels of lipogenic genes (*Cpt-1*, *Ppara* and *Srebp1-c*) were significantly increased in the livers of H, CD and HCD mice (Joshi et al., 2021). In parallel, HepG2 cells were treated with 0.5 mM of oleic acid (OA) for 24 hours to induce fatty changes. Inducing intracellular lipid accumulation by subjecting hepatocytes to saturated fatty acids such as palmitic acid (PA) (Joshi-Barve et al., 2007)(Upadhyay et al., 2020), OA (Joshi et al., 2021)or a combination of both (Y. Sun et al., 2021)is a widely employed approach and has been extensively studied in our laboratory.

The CLOCK: BMAL1 heterodimer plays a crucial role in regulating hepatic lipid metabolism by interacting with key lipid metabolism genes such as *Srebp1-c* (Bideyan, 2022)and *Ppara* (Luo et al., 2023). Previous studies from our laboratory had reported that the liver tissues of H and/or CD mice exhibited expression of *Srebp1-c* and *Ppara* (Joshi et al., 2021). Similarly, studies have demonstrated that the transcription of the human *NOCT* gene is controlled by the CLOCK: BMAL1 heterodimer through the E-box of the *NOCT* promoter. Moreover, it was revealed

that E-box2, in particular, was more efficient than E-box1 in regulating CLOCK: BMAL1 mediated *NOCT* transcription *in vitro* (Li et al., 2008). It was further reported that increased *Noct* expression at night was driven by the binding of phosphorylated cAMP response element-binding protein (pCREB) to the Nocturnin Element (NE; GTGACGTG) within the Noct promoter in *Xenopus* retina. During the day, light inhibits CREB phosphorylation, whereas nighttime darkness promotes pCREB production, thus activating *Noct* transcription (Liu & Green, 2002a). Additionally, studies had shown that *Noct* mRNA expression was significantly decreased in mice homozygous for a hypomorphic *Clock* allele (Liu & Green, 2002b; Oishi et al., 2003), implying that CLOCK regulates *Noct* expression, either directly or indirectly.

In the current study, we observed significant alterations in the oscillatory patterns of hepatic *Noct* mRNA in H and/or CD mice, with CD and HCD groups showing maximal variations, and the H group exhibiting consistently elevated expression at all time points. Hepatic *Noct* oscillations in control and H-diet-fed mice are consistent with previously published reports (Stubblefield et al., 2018) . Interestingly, the impact of circadian desynchrony (CD) alone, or in combination with H diet (HCD), on *Noct* rhythmicity has not yet been explored, making this aspect of our study novel.

In line with our *in vivo* findings, HepG2 cells treated with 0.5 mM of oleic acid (OA) also recorded significant increment and disruptions in Noct mRNA and protein oscillations. A notable increment in *NOCT* mRNA was observed at 36 h, whereas NOCT protein oscillations shifted from a peak at 48 h (in control cells) to 32 h in OA-treated cells. The oscillations of Noct in control HepG2 cells align with previous reports wherein; Noct expression peaked at 36 h and ~48 h, respectively, in primary cultures of mouse embryonic fibroblasts (MEFs) (Niu et al., 2011). CircWave analysis confirmed significant increases in relative amplitude and shifts in the centre of gravity (CoG). Interestingly, while cumulative *NOCT* expression was significantly higher in the OA group, NOCT protein levels revealed a moderate decrement. Noct has been extensively studied in HepG2 cells, particularly in terms of its localization and function. However, its role in MASLD

has not been previously investigated and our study provides evidence linking altered Noct oscillations to the pathophysiology of the said disease.